

A Hyperbranched Copolymer of Poly(dialkoxy-*p*-phenylenevinylene) and Trivinylenebenzene Units: Synthesis, Characterization, Photo- and Electroluminescence Properties

Hualin Wang,[†] Yueming Sun,^{*,†} Zhengjian Qi,[†] Fan Kong,[†] Yongquan Ha,[†] Shougen Yin,[‡] and Shen Lin[‡]

School of Chemistry and Chemical Engineering, Southeast University, Nanjing 210096, P. R. China, and Institute of Material Physics, Tianjin University of Technology, Tianjin 300384, P. R. China

Received December 12, 2007; In Final Form March 14, 2008;

Revised Manuscript Received March 11, 2008

ABSTRACT: A novel hyperbranched copolymer, poly(2,4,6-tributyloxy-1,3,5- trivinylenebenzene-*co*-2-methoxy-5-octyloxy-*p*-phenylenevinylene) PTBOTV-*co*-PMOPV, and a linear counterpart poly(2-methoxy-5-octyloxy-*p*-phenylenevinylene) (PMOPV) were synthesized by the Gilch polymerization and characterized with UV–vis, FT-IR, ¹H NMR and Photoluminescence (PL) spectroscopy. PTBOTV-*co*-PMOPV showed excellent solubility, good film-formation ability, and high thermal stability. The UV–vis, PL, and electroluminescence (EL) spectra of PTBOTV-*co*-PMOPV were blue-shifted approximately 9–15 nm on comparison with those of PMOPV. The polymer light-emitting diode (PLED) was fabricated in ITO/PEDOT (50 nm)/polymer (60 nm)/Alq₃ (30 nm)/LiF (1 nm)/Al (200 nm) configuration. The PTBOTV-*co*-PMOPV exhibited the maximum external quantum efficiency (EQE) of 0.26% at 60.7 cd/m², while the PMOPV device showed the maximum EQE of 0.17% at 88 cd/m².

Introduction

Since the first poly(*p*-phenylenevinylene) (PPV) was reported by the Cambridge group in 1990,¹ the synthesis and applications for polymer light-emitting diodes of PPV derivatives (PPVs) have attracted more attention because of their easily adjustable structures, excellent properties of the light–electric interconversion, and good mechanical properties.^{2,3} Great effects have been made to design novel PPVs containing different kinds of side-chain or main-chain for various applications such as absorption spectrum, quantum yield, and optical band gap energy (*E_g*).⁴ Poly(dialkoxy-*p*-phenylenevinylene)s (OPVs) and its derivatives are attractive in conjugated polymers since alkoxy substitutions at the 2,5-hydrogens of the phenyls make them possess remarkable properties such as solubility and processability.⁵ It is a general trend that the band gaps of PPV derivatives are reduced as electron donating alkoxy groups are attached to phenylene rings of PPV, and then the wavelength of the emitted light is red-shifted, so most of the poly(dialkoxy-*p*-phenylenevinylene)s show emissions in the red–orange region.^{6–8} The intermolecular interactions of the linear PPVs, such as aggregation and excimer formation, will lead to red-shift, reduction in color purity, and reduced efficiency in emission.^{9–11} Branching of *p*-conjugated systems can be designed to reduce aggregation tendency and to define the color of the emitting light.^{12,13} However, it is very difficult to obtain the dendritic systems because of the complicated synthesis procedure and low yield.¹⁴ But for hyperbranched polymers, a transitional structure of linear polymer and dendrimers with many branches on their molecular backbones can be synthesized much easier even in a single step compared to dendrimers.^{15,16} Three-dimensional hyperbranched polymer always has an asymmetric or irregular structure and shows lower intrinsic viscosity, better processability, and more tunable emission color than linear polymers.¹⁷ In addition, the hyperbranched polymers can

improve the morphologies of the thin films and prevent crystallization.¹⁸

Different synthetic strategies have been employed for the preparation of the hyperbranched polymers by using different core connecting units and terminal groups.^{19–21} In the present work, we used tributylxybenzene vinylene as the core to synthesize the hyperbranched polymers via the Gilch route.²² We report the synthesis, electroluminescence, and photovoltaic properties of a linear poly(dialkoxy-*p*-phenylenevinylene) and its hyperbranched copolymer. The obtained polymers, PTBOTV-*co*-PMOPV and PMOPV, have large molecular weights and high thermal stabilities and are easily applicable for PLEDs. The presence of trivinylenebenzene units in the main chain was found to improve the solubility and aided in tuning the luminescent and photovoltaic properties.

Experimental Section

Materials. Phloroglucin, 4-methoxyphenol, 1-bromooctane, butyl bromide, potassium tert-butoxide were purchased from Aldrich Chemical Co. (NJ). Paraformaldehyde, *N,N*-dimethylformamide, chloroform, tetrahydrofuran (THF), and other reagents/solvents were analytic-grade quality and were purified by following the standard procedures before use. 1-Methoxy-4-octyloxybenzene and 1,4-bis(chloromethyl)-2-methoxy-5-octyloxybenzene were synthesized according to the literature method.²³ PMOPV was synthesized via a typical Gilch polymerization as shown in scheme 1.

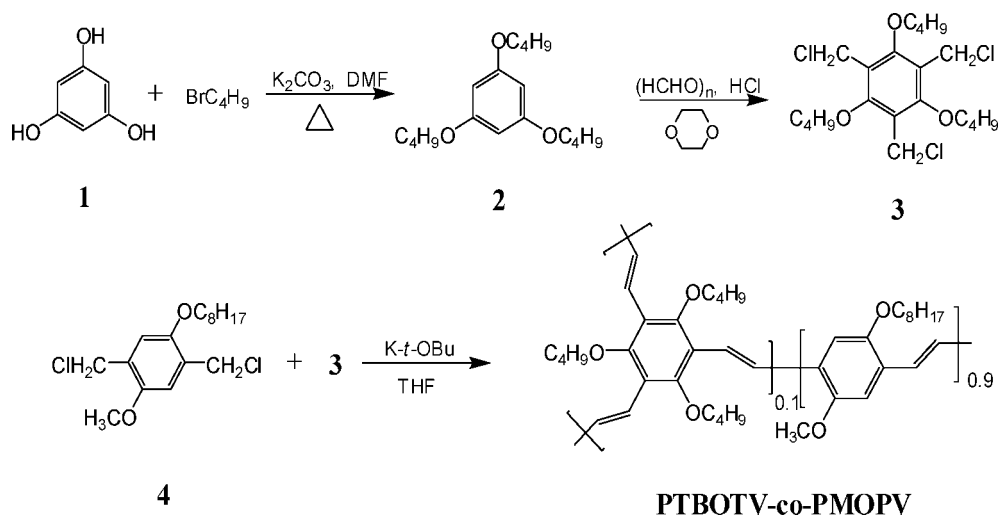
General Methods. ¹H and ¹³C NMR spectra of the compounds and polymers were recorded on a 300 MHz Bruker NMR spectrophotometer in CDCl₃ at room temperature, containing a small amount of TMS as internal standard. Infrared spectra of the samples were recorded with a Nicolet 700 Fourier transform infrared (FT-IR) spectrophotometer in the solid state. High-performance liquid chromatography (HPLC) was performed on a Perkin-Elmer instrument using Spheri-5 RP-18 column (4.6 × 250 mm i.d., 5 μm coating), and the compounds were eluted with methanol and detected by a UV spectrophotodetector at 254 nm. Elemental analyses were performed with

* Corresponding author. E-mail: sun@seu.edu.cn. Fax +86-25-52090621.

[†] Southeast University.

[‡] Tianjin University of Technology.

Scheme 1. Synthetic Routes of Monomers and Copolymer



Elementar Vario MICRO. The molecular weights of the polymers were determined by gel permeation chromatography (GPC) using a Perkin-Elmer series 200 apparatus in THF with polystyrene as standards. The flow rate of THF was maintained as 1.0 mL/min at 40 °C. The thermal stability of the polymers was determined using a DuPont 9900 analyzer at a heating rate of 10 °C/min in nitrogen atmosphere. The absorption and emission studies were done using a UV-2201 UV-vis spectrophotometer and a Spex (NJ) FL-2T2 spectrofluorometer. The solution spectra were recorded in chloroform, while the solid-state spectra were obtained from polymer thin films prepared by spin-casting the chloroform solutions on glass substrates. The PL quantum yields (ϕ_{PL}) of the polymers in chloroform were determined by comparison to quinine sulfate in 0.10 M H_2SO_4 as standard.²⁴

Fabrication and Characterization of Light-Emitting Devices. Polymer LED devices were fabricated with the configuration ITO/PEDOT(50 nm)/polymer(60 nm)/Alq₃(30 nm)/LiF(1 nm)/Al(200 nm). The device schematic diagram is shown in Figure 5. The ITO glass was cleaned as described in other literature.²⁵ A 50 nm thick hole injection layer of poly(ethylenedioxythiophene) (PEDOT) doped with poly(styrenesulfonate) (PSS) was spin coated on the top of ITO substrate from a 0.7 wt % dispersion in water and then dried in vacuum at 150 °C for 1 h. The light-emitting layer was spin coated on the top of the PEDOT layer by using chloroform as the solvent and then dried for 3 h at 60 °C in vacuum. The Alq₃ layer was grown by thermal sublimation in vacuum at 3×10^{-6} Torr. The Alq₃ layer was used as the electron transport layer to block holes and confine excitons.²⁶ To improve electron injection, a thin layer of lithium fluoride (LiF) was evaporated at a rate of 0.1 nm/s. Finally, a 200 nm thick aluminum cathode was slowly evaporated onto the substrate at a rate of 1 nm/s. The active area of each EL device was 0.2 cm². Electroluminescence spectra were measured with a Minolta CS-1000. The current/voltage and luminescence/voltage characteristics were measured by a current/voltage source (Keithley 2400) and a luminescence detector (Minolta PR-650). External quantum efficiencies were calculated by using a standard expression involving the measured ratio of forward directed luminance and device current density, taking into account the EL spectral distribution and the photopic spectrum.

1,3,5-Tributylloxybenzene (2). Phloroglucin (**1**) (3.9 g, 0.03 mol), *N,N*-dimethylformamide (200 mL), anhydrous potassium carbonate (25 g, 0.18 mol), and 18-crown-6 (7.9 g, 0.03 mmol) were added to a round-bottom flask under N₂ atm. Butyl

bromide (10 mL, 0.09 mol) was then added dropwise over a period of 0.5 h. The mixture was stirred at room temperature for 20 h and then heated to reflux for 2 h. DMF and the excess butyl bromide were removed by reduced pressure. By dissolving the mixture in 100 mL chloroform and 200 mL water, washing the organic layer successively with brine solution, drying it with anhydrous magnesium sulfate, and then further purifying with a silica gel column using 10:1 of petroleum ether:ethyl acetate as eluent, the desired pure product **2** was obtained as a beige liquid (5.6 g, 61% yield). ¹H NMR (CDCl_3) δ : 6.08 (s, 3H, Ar-H), 3.90 (t, 6H, O-CH₂), 1.75 (m, 6H, CH₂), 1.47 (m, 6H, CH₂), 0.96 (t, 9H, CH₃). FT-IR (cm^{-1}): 3011.2, 2958.3, 2933.2, 2871.5, 1731.8, 1598.7, 1463.7, 1384.7, 1259.3, 1070.3, 1166.7, 817.7, 680.8. Anal. Calcd for $\text{C}_{18}\text{H}_{27}\text{O}_3$: C, 74.23; H, 9.28. Found: C, 73.98; H, 9.45.

1,3,5-Trichloromethyl-2,4,6-tributylloxybenzene (3). A mixture of 1,3,5-tributylloxybenzene (**2**) (4.5 g, 0.015 mol), paraformaldehyde (1.6 g, 0.05 mol), *p*-dioxane (100 mL), formaldehyde solution (1 mL), and concentrated hydrochloric acid (30 mL) was stirred at room temperature. Sufficient HCl was continually inflated into the solution to keep the concentration of dissolved HCl constant, and the mixture was stirred for 10 h. It was subsequently concentrated under reduced pressure, and then 150 mL chloroform was added to the concentrate. The organic layer was successively washed with water and brine solution, dried over anhydrous magnesium sulfate, and further purified with a silica gel column using 5:1 of petroleum ether:ethyl acetate as eluent. The obtained product **3** was a brown rosy liquid (4.8 g, 72% yield). ¹H NMR (CDCl_3) δ : 4.71 (s, 6H, -CH₂Cl), 3.71 (t, 6H, O-CH₂), 1.31–1.82 (m, 12H, CH₂), 1.01 (t, 9H, CH₃). FT-IR (cm^{-1}): 2958.3, 2933.2, 2871.5, 1729.9, 1581.4, 1465.7, 136.7, 1378.9, 1267.0, 1184.1, 1097.3, 1020.2, 665.3. Anal. Calcd for $\text{C}_{21}\text{H}_{30}\text{O}_3\text{Cl}_3$: C, 57.73; H, 6.87. Found: C, 57.48; H, 7.02.

Synthesis of Polymers. A typical polymerization procedure of PTBOTV-co-PMOPV (**4**) is described as following. A solution of 8.4 mL of potassium *tert*-butoxide (2.0 M THF solution, 16.8 mmol) was slowly added over 1 h to a stirred solution of **3** (0.09 g, 0.2 mmol) and 1,4-bis(chloromethyl)-2-methoxy-5-octyloxybenzene (0.6 g, 1.8 mmol) in 25 mL dry THF that was cooled to -5 °C, and a N₂ atmosphere was maintained. The viscosity of the mixture gradually increased with orange-red fluorescence and the mixture was stirred at room temperature for 20 h. The polymerization solution was poured into 500 mL MeOH. A crude polymer precipitated out, which was redissolved in chloroform and reprecipitated from MeOH and then extracted

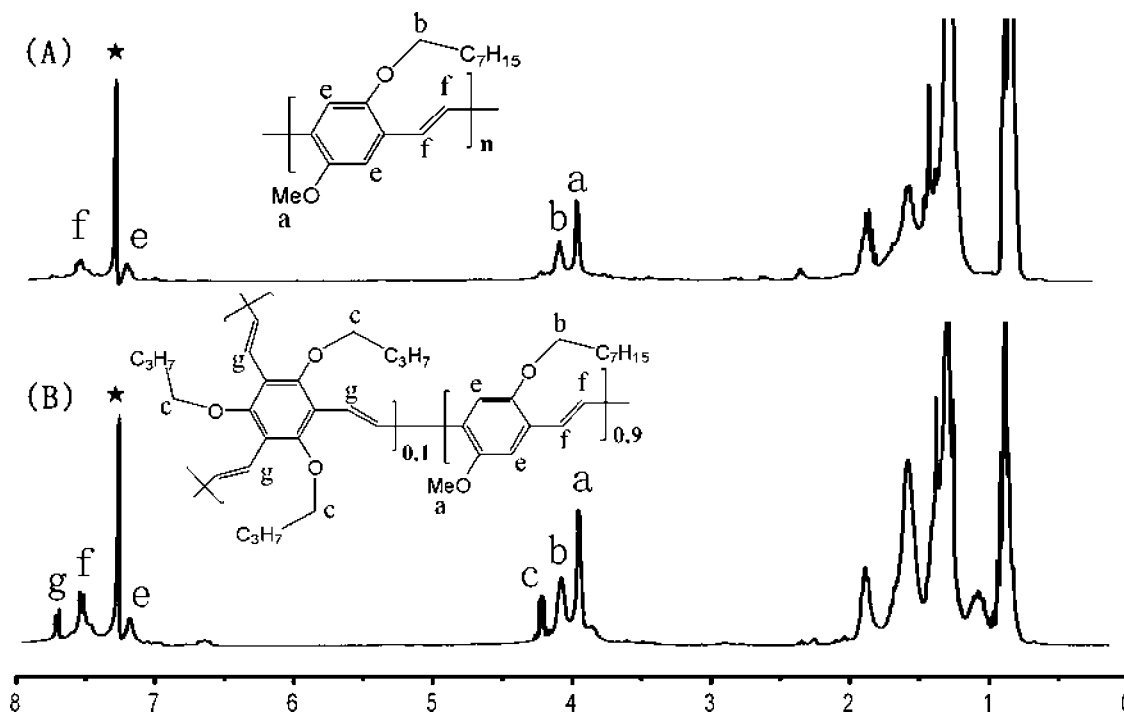


Figure 1. ^1H NMR spectra of PMOPV (A) and PTBOTV-*co*-PMOPV (B) in CDCl_3 . The peaks indicated by asterisk are corresponding to CHCl_3 in CDCl_3 .

Table 1. Physical Properties of the Polymers

polymer	TBOTVB monomer in feed (mol %)	TBOTVB amount in copolymers (mol %)	yield (%)	M_n	M_w	<i>PDI</i>	T_d^a ($^\circ\text{C}$)
PMOPV	0	0	56	35 000	126 000	3.6	355
PTBOTV- <i>co</i> -PMOPV	10	12.3	48	75 000	239 000	3.2	336

^a Temperature resulting in 5% weight loss based on initial weight.

by Soxhlet with MeOH to remove the impurities and oligomers. After filtration and drying in vacuum, a bright red fibrous polymer, PTBOTV-*co*-PMOPV (10:90 mol %), was obtained. FT-IR (cm^{-1}): 3058.6, 2991.1, 2927.5, 2854.2, 1735.6, 1589.1, 1504.2, 1463.7, 1351.9, 1255.5, 1205.3, 1122.4, 1041.4, 968.1, 854.3.

PMOPV (**5**) was obtained from 1,4-bis(chloromethyl)-2-methoxy-5-octyloxybenzene with a similar procedure as that described for PTBOTV-*co*-PMOPV. The yield of a bright red solid (PMOPV) was 56%. ^1H NMR (CDCl_3) δ : 7.5 (m, 2H, $\text{CH}=\text{CH}$), 7.2 (s, 2H, Ph-H), 4.1 (t, 2H, OCH_2), 3.9 (s, 3H, OCH_3), 1.8–0.9 (m, 12H, CH_2), 0.8 (t, 3H, CH_3). ^{13}C NMR (CDCl_3) δ : 151.4, 127.4, 123.4, 110.9, 109.1, 69.7, 56.4, 32.2, 29.5, 26.4, 22.7, 14.1. FT-IR (cm^{-1}): 3058.6, 2991.1, 2925.5, 2854.2, 1735.6, 1596.8, 1502.3, 1463.7, 1413.6, 1351.9, 1205.3, 1041.4, 968.1, 854.3, 696.2. Anal. Calcd for $[\text{C}_{17}\text{H}_{24}\text{O}_2]_n$: C, 80.63; H, 9.48. Found: C, 78.68; H, 9.28.

Results and Discussion

Synthesis and Characterization of Polymers. The general synthetic routes of the monomers and the polymers are outlined in scheme 1. In the first step, phloroglucin (**1**) was coupled with butyl bromide using potassium carbonate in DMF to generate 1,3,5-tributylloxybenzene (**2**), which was chloromethylated with paraformaldehyde and HCl in *p*-dioxane to provide 1,3,5-trichloromethyl-2,4,6-tributylloxybenzene (**3**). The structures and purities of the monomers were confirmed by ^1H NMR. The copolymer and homopolymer were prepared by the Gilch polymerization with an excess amount of potassium *tert*-butoxide in THF under N_2 atmosphere.

The ^1H NMR spectra of PMOPV (A) and PTBOTV-*co*-PMOPV (B) are shown in Figure 1. The various types of alkoxy

protons, aromatic protons and vinylic protons are assigned by letters. Previous studies show that the alkoxy protons of the OPVs are significantly difference in the ^1H NMR spectra, and the chemical shift values of the $\text{Ar}-\text{OCH}_2-$ protons are highly sensitive to their structural difference.^{27,28} According to this, the two types of repeating units in the hyperbranched copolymers can be distinguished by their structural variation. In the PMOPV repeating unit, the alkoxy protons corresponding to the $\text{Ar}-\text{OCH}_3$ (type a) are well separated from the $\text{Ar}-\text{OCH}_2-$ protons (type b). A new triplet located at 4.24–4.22 ppm attributed to the $\text{Ar}-\text{OCH}_2-$ protons (type c) in PTBOTV repeating unit was observed in Figure 1B, suggesting that PTBOTV-*co*-PMOPV copolymer has been successfully formed. Similarly, at 7.73–7.69 ppm, there was observed a new multiplet from the vinylic protons (type g) near the benzene ring of the PTBOTV repeating unit, which was clearly separated from the PMOPV unit protons (type f). These observations are consistent with their chemical structures. Therefore, the composition ratios of PTBOTV (12.3 mol %) can be calculated from the integration ratios of 7.73–7.69 and 4.24–4.22 ppm peaks of the ^1H NMR spectra.

Table 1 summarizes the comparison of the two polymers. The two polymers are soluble in common organic solvents such as chloroform, THF, dichloromethane. The solubility of PTBOTV-*co*-PMOPV is much better than that of PMOPV in these common solvents since it possesses a more branched and compact global structure, which make the intermolecular interactions smaller than its linear counterparts and thus increase the solubility.²⁹ The thermogravimetric analysis showed that the present polymers have good thermal stabilities with 5 wt % loss at 336 $^\circ\text{C}$ for PTBOTV-*co*-PMOPV and at 355 $^\circ\text{C}$ for PMOPV. The glass transition temperature of the polymers could not be

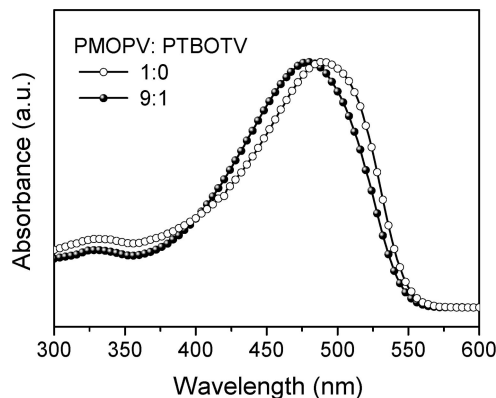


Figure 2. Absorption spectra of PMOPV and PTBOTV-co-PMOPV in CHCl_3 solution.

identified by differential scanning calorimetry (DSC). This can be ascribed to the rigidity of their main chains. The number-average molar mass (M_n) determined by GPC analysis was found to be 75×10^3 for PTBOTV-co-PMOPV and 35×10^3 for PMOPV. The polydispersity indices of the two polymers PTBOTV-co-PMOPV and PMOPV were 3.2 and 3.6, respectively.

Optical Properties of Polymers. Figure 2 shows the UV-vis absorption spectra of PTBOTV-co-PMOPV and PMOPV in chloroform. The absorption peak of PMOPV is at 492 nm, while the absorption peak of PTBOTV-co-PMOPV is blue-shifted to 478 nm. The phenomenon is the same as those found in other hyperbranched conjugated polymers.^{21,30,31} The results indicated that the introduced tributylxybenzene groups decrease the average conjugation length of the copolymer. Normally, if the two adjacent monomer units in conjugated polymers have different symmetries and orbital energies, the electron coupling will be reduced and then the conjugation is destroyed.^{32,33} In the homopolymer, all the monomer units are nearly coplanar to make the electronic coupling maximum between adjacent monomer units. Obviously, the tributylxyphenylenevinylene (TBOTV) unit has different symmetry and orbital energy compared to the 2-methoxy-5-octyloxy-phenylenevinylene (MOPV) unit in the copolymer. In addition, alkoxy groups in the TBOTV units can increase steric hindrance effect. So, the TBOTV units introduced into the copolymer backbone destroy the coplanar conformation. As a result, the π -electron delocalization is restricted in the copolymer chains with nonplanar conformations resulting in shorter conjugation, and hence the blue-shifted absorption peak is observed in PTBOTV-co-PMOPV. The UV-vis absorption spectra indicate that the optical band gaps of PTBOTV-co-PMOPV and PMOPV are nearly the same. This indicates that some of the long conjugation segments of the copolymer are same as those of PMOPV. Since the tributylxybenzene groups are introduced into the copolymer chains at random, some of the long conjugation segments could still remain.

Figure 3 shows the PL spectra of PTBOTV-co-PMOPV and PMOPV in chloroform and films. The PL peaks of the two polymer solutions are at 555 nm, corresponding to their absorption edges. In dilute solutions, the polymer chains are separated by solvent. The conjugations of the polymers are obviously affected by the solvents due to their different chain conformations in the different solvents.³⁴ Normally, emissions originate from the radiative recombination of excitons in long segments with low energies in conjugated polymers. As the polymers are excited at 480 nm, the excitons in short segments are formed and then transferred to long segments until they become trapped at a low-energy site, from which the emission occurs.³⁵ The PL spectra of the polymer films were obtained

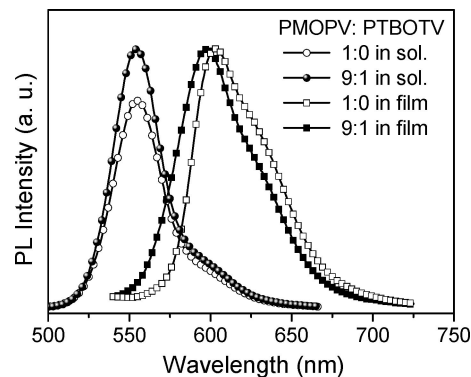


Figure 3. Photoluminescence spectra of the polymers in CHCl_3 solutions (excitation at 480 nm) and films (excitation at 500 nm).

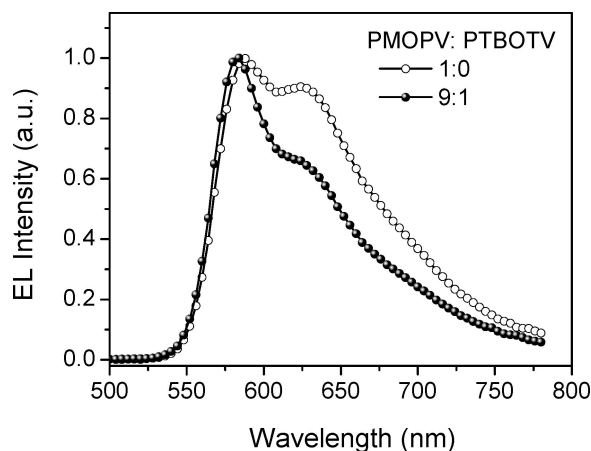


Figure 4. Electroluminescence spectra of the polymers in devices of configuration ITO/PEDOT/polymer/Alq₃/LiF/Al.

by excitation at 500 nm. Obviously, the PL peak of the PTBOTV-co-PMOPV film is blue-shifted by comparison with the PMOPV film. Different from PMOPV, the steric and nonplanar structure of PTBOTV-co-PMOPV hinder the aggregation of the polymer chains to result in weak interchain interactions in films.³⁰ As we know, the interchain interactions widen the energy bands of the conjugated polymers to reduce their optical energy gaps. The larger interchain interactions in the PMOPV film make its optical energy gap less than that of the PTBOTV-co-PMOPV film. As a result, the blue-shifted PL spectrum was observed in the copolymer film. PTBOTV-co-PMOPV as a hyperbranched polymer has a high steric structure,³⁶ which could hinder the nonradiative process of its singlet excited state to gain an obviously higher PL quantum yield of 0.43 compared to 0.24 for PMOPV.

Electroluminescence Properties of LED Devices. The PLED devices based on the two polymers with the configuration of ITO/PEDOT (50 nm)/polymer (60 nm)/Alq₃ (30 nm)/LiF (1 nm)/Al (200 nm) were fabricated to investigate the electroluminescent properties. As shown in Figure 4, the EL spectra of PTBOTV-co-PMOPV and PMOPV show maximum peaks at 582 and 588 nm, respectively. These features are similar to those observed in the PL spectra of the corresponding polymer films, which indicate that both the PL and EL originate from the same radiative decay process of the singlet exciton. Different from the PL spectra of the films, the EL spectra show obvious shoulder peaks near at 625 nm. It has been found that the relative intensity of the EL shoulder peak of PMOPV is larger than that of PTBOTV-co-PMOPV. Such shoulder peak is usually considered to be connected with interchain interactions, so the lower EL shoulder peak further indicates that the hyperbranched

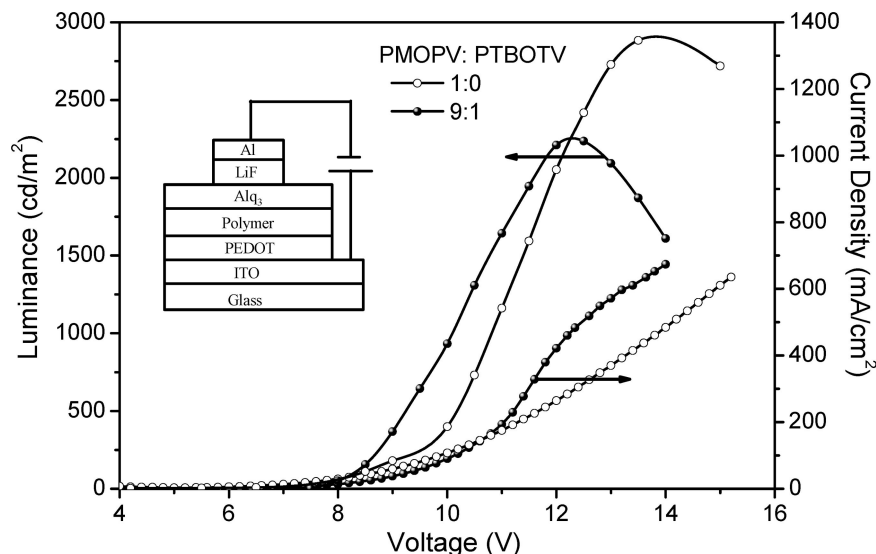


Figure 5. Current–voltage (J - V) and luminescence–voltage (L - V) characteristics of the PLEDs devices of configuration ITO/PEDOT/polymer/ Alq_3 /LiF/Al. The inset shows the device schematic.

Table 2. Performances of Devices Having Structures ITO/PEDOT/Polymer/ Alq_3 /LiF/Al

device	PMOPV	PTBOTV- <i>co</i> -PMOPV
turn-on voltage (V) ^a	4.2	5.3
voltage (V) ^b	9.9	10.1
external quantum efficiency (%) ^b	0.15	0.24
max brightness (cd/m^2)	2916 (at 13.7 V)	2246 (at 12.3 V)
max external quantum efficiency (%)	0.17	0.26
EL (nm) ^c	588 (625)	582 (625)

^a At 1 cd/m^2 . ^b At 100 mA/cm^2 . ^c At 7 V.

structure of PTBOTV-*co*-PMOPV hinder the aggregation of the polymer chains. The electroluminescent properties of the PLEDs based on the polymers are summarized in Table 2

Figure 5 shows current density–voltage and luminescence–voltage characterization of the PLED devices. The current density increased exponentially with the increasing forward bias voltage, which is a typical diode characterization. The turn-on voltage of the PLEDs based on PTBOTV-*co*-PMOPV and PMOPV were approximately 5.3 and 4.2 V, respectively. The maximum luminescence (L_{max}) of PMOPV is 2916 cd/m^2 at 13.7 V. However, the maximum luminescence of PTBOTV-*co*-PMOPV dramatically decreased to about 2246 cd/m^2 at a voltage of 12.3 V. Figure 6 shows the dependence of external quantum efficiency on the current density for the two LED devices. The maximum external quantum efficiency of the PTBOTV-*co*-PMOPV device is about 0.26%, significantly higher than that of the other polymer device (0.17%).³⁷ At present, there is no clear explanation for the disparity between the external quantum efficiencies of hyperbranched and linear polymers. It is supposed that the higher external quantum efficiency of PTBOTV-*co*-PMOPV may be due to the enhancement of the charge transport channel (mainly for holes) along the PPV backbone as well as easier hole injection in this system.

Conclusions

We have successfully synthesized a novel hyperbranched copolymer PTBOTV-*co*-PMOPV with trivinylphenylene units in the backbone via Gilch reaction. On comparison with PMOPV, PTBOTV-*co*-PMOPV has good solubility in common organic solvents. The absorption maximum of PTBOTV-*co*-PMOPV is blue-shifted on comparison with PMOPV due to its steric and nonplanar structure. The copolymer has an obviously

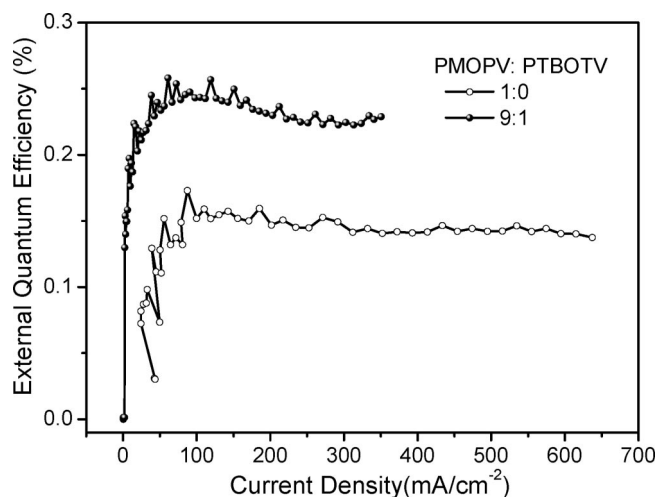


Figure 6. External quantum efficiency vs current density characteristics in devices of configuration ITO/PEDOT/polymer/ Alq_3 /LiF/Al.

higher PL quantum yield of 0.43 as compared to 0.24 for the homopolymer. The devices with configuration ITO/PEDOT (50 nm)/polymer (60 nm)/ Alq_3 (30 nm)/LiF (1 nm)/Al (200 nm) have been fabricated, and the initial result show that PTBOTV-*co*-PMOPV can be potentially used in PLEDs.

Acknowledgment. We thank the support of the National Key Project on Basic Sciences (2007CB936300) and the High-Technique Project Foundation of Jiangsu Province (BG 2006033).

Note Added After ASAP Publication. This article was published ASAP on April 18, 2008. During production, middle initials were added to authors' names in error. These initials have been removed. The correct version was published on April 22, 2008.

References and Notes

- (1) Burroughes, J. H.; Bradley, D. D. C.; Brown, A. R.; Marks, R. N.; Mackay, K.; Friend, R. H.; Burns, P. L.; Holmes, A. B. *Nature (London, U.K.)* **1990**, *347*, 539.
- (2) Bernius, M. T.; Inbasekaran, M.; O'Brien, J.; Wu, W. *Adv. Mater.* **2000**, *23*, 1737.
- (3) Brunner, K.; Langeveld-Voss, B. M. W.; Schoo, H. F. M.; Hofstraat, J. W. *J. Phys. Chem. B* **2002**, *106*, 6834.

- (4) Madhugiri, S.; Dalton, A.; Gutierrez, J.; Ferraris, J. P.; Balkus, K. *J. Am. Chem. Soc.* **2003**, *125*, 14531.
- (5) Cacialli, F.; Chuah, B. S.; Friend, R. H.; Moratti, S. C.; Holmes, A. B. *Synth. Met.* **2000**, *111*, 155.
- (6) Braun, D.; Heeger, A. J. *Appl. Phys. Lett.* **1991**, *58*, 1982.
- (7) Bradley, D. D. C. *Adv. Mater.* **1992**, *4*, 756.
- (8) Anderson, M. R.; Yu, G.; Heeger, A. J. *Synth. Met.* **1997**, *85*, 1275.
- (9) Chu, H. Y.; Hwang, D. H.; Do, L. M.; Chang, J. H.; Shim, H. K.; Holmes, A. B. *Synth. Met.* **1999**, *101*, 216.
- (10) Hsieh, B. R.; Yu, Y.; Forsythe, E. W.; Schaaf, G. M.; Feld, W. A. *J. Am. Chem. Soc.* **1998**, *120*, 231.
- (11) Peng, Z.; Zhang, J.; Xu, B. *Macromolecules* **1999**, *32*, 5162.
- (12) Precup-Blaga, F. S.; Garcia-Martinez, J. C.; Schenning, A. P. H. J.; Meijer, E. W. *J. Am. Chem. Soc.* **2003**, *125*, 12953.
- (13) Kwon, T. W.; Alam, M. M.; Jenekhe, S. A. *Chem. Mater.* **2004**, *16*, 4657.
- (14) Scott, M. G.; Frechet, J. M. J. *Chem. Rev.* **2001**, *101*, 3819.
- (15) Frechet, J. M. J. *Science* **1994**, *263*, 1710.
- (16) Kim, Y. H.; Webster, O. W. *Macromolecules* **1992**, *25*, 5561.
- (17) Wooley, K. L.; Frechet, J. M. J.; Hawker, C. J. *Polymer* **1994**, *35*, 4489.
- (18) Matthew, R. R.; Wang, S.; Guillermo, C. B.; Cao, Y. *Adv. Mater.* **2000**, *12*, 1701.
- (19) Voit, B. J. *Polym. Sci., Part A: Polym. Chem.* **2000**, *38*, 2505.
- (20) Inoue, K. *Prog. Polym. Chem.* **2000**, *25*, 453.
- (21) Tsai, L. R.; Chen, Y. *Macromolecules* **2007**, *40*, 2984.
- (22) Gilch, H. G.; Wheelwright, W. L. *J. Polym. Sci., Part A* **1966**, *4*, 1337.
- (23) Amrutha, S. R.; Jayakannan, M. *J. Phys. Chem. B* **2006**, *110*, 4083.
- (24) Demas, J. N.; Crosby, G. A. *J. Phys. Chem.* **1971**, *75*, 991.
- (25) Chung, S. J.; Kwon, K. Y.; Lee, S. W.; Jin, J. I.; Lee, C. H.; Lee, C. E.; Park, Y. *Adv. Mater.* **1998**, *10*, 1112.
- (26) Culligan, S. W.; Geng, Y.; Chen, S. H.; Klubek, K.; Vaeth, K. M.; Tang, C. W. *Adv. Mater.* **2003**, *15*, 1176.
- (27) Amrutha, S. R.; Jayakannan, M. *Macromolecules* **2007**, *40*, 2380.
- (28) Liu, Y.; Yang, C. H.; Li, Y. J.; Li, Y. L.; Wang, S. *Macromolecules* **2005**, *38*, 716.
- (29) Ohnishi, T.; Doi, S.; Tsuchida, Y. *IEEE Trans. Electron Devices* **1997**, *44*, 1253.
- (30) Ding, L.; Bo, Z.; Chu, Q.; Li, J.; Dai, L.; Pang, Y.; Karasz, F. E.; Durstock, M. F. *Macromol. Chem. Phys.* **2006**, *207*, 870.
- (31) Tsai, L. R.; Chen, Y. J. *Polym. Sci., Part A: Polym. Chem.* **2007**, *45*, 4465.
- (32) Chen, L. X.; Jalger, W. J. H.; Niemczyk, M. P.; Wasielewski, M. R. *J. Phys. Chem. A* **1999**, *103*, 4341.
- (33) Kong, F.; Wu, X. L.; Huang, G. S.; Yuan, R. K.; Yang, C. Z.; Chu, P. K.; Siu, G. G. *Appl. Phys. A: Mater. Sci. Process.* **2006**, *84*, 203.
- (34) Nguyen, T. Q.; Doan, V.; Schwartz, B. J. *J. Chem. Phys.* **1999**, *110*, 4068.
- (35) Guha, S.; Rice, J. D.; Yau, Y. T.; Martin, C. M.; Chandrasekhar, M.; Chandrasekhar, H. R.; Guentner, R.; Scanducci de Freitas, P.; Scherf, U. *Phys. Rev. B* **2003**, *67*, 125204.
- (36) Andersson, M. R.; Yu, G.; Heeger, A. J. *Synth. Met.* **1997**, *85*, 1275.
- (37) Li, X. Z.; Zeng, W. J.; Xia, Y. J.; Yang, W.; Cao, Y. *J. Appl. Polym. Sci.* **2006**, *102*, 4321.

MA702774X